**Text S1:**

The calibrated parameters and their respective values for each basin are presented in Table S4. These parameters influence several key physical processes that control the hydrological response. Infiltration is regulated by the parameters bexp, smcmax, dksat, and refkdt, where higher values of these parameters generally lead to increased infiltration. Soil evaporation, on the other hand, is primarily governed by rsurfexp and smcmax, with elevated values of both promoting higher soil evaporation rates.

Aquifer recharge is strongly affected by the slope parameter. Lower values of slope reduce the transfer of water from the soil column to the groundwater reservoir, thereby decreasing aquifer recharge. Similarly, baseflow is influenced by zmax, expon, and coeff. High values of zmax tend to suppress baseflow contributions to river discharge, while higher values of expon and coeff increase it.

Transpiration processes are controlled by the parameters cwpvt, mp, vcmx25, and hvt. A decrease in cwpvt leads to higher transpiration rates, whereas lower values of mp, vcmx25, and hvt result in reduced transpiration. Overland flow routing, which is affected by retdeprtfac and ovroughrtfac, decreases with higher values of these parameters. Subsurface flow is governed by lksatfac, where an increase in its value enhances subsurface water movement.

The calibration process revealed some notable overall trends across all basins. There was a consistent increase in refkdt, which controls runoff partitioning and results in a higher proportion of subsurface runoff compared to surface runoff. Additionally, the slope parameter consistently decreased, reducing deep drainage from the soil column to the groundwater reservoir. The zmax parameter showed a general increase across most basins, except for Göksu, leading to reduced baseflow contributions to river discharge.

While these three parameters exhibited relatively uniform behaviour across all basins, others displayed more variable trends. For instance, parameters such as bexp, smcmax, dksat, and rsurfexp showed both increases and decreases depending on the basin, reflecting local hydrological conditions.

This variability underscores the complexity of the calibration process. The interplay between parameters often determines the final hydrological outcome, as the effect of one parameter can be moderated or even compensated by another influencing the same physical process. In some cases, one parameter may dominate over others, masking their effects. These findings highlight the importance of considering the combined influence of multiple parameters to ensure accurate and balanced calibration for hydrological modelling.

**Text S2:**

To investigate the influence of meteorological forcing errors, we assessed the performance of WRF precipitation input by calculating the mean daily percent bias relative to EOBS precipitation data for each basin (Figure S7).

The results reveal a mixed pattern of biases, ranging from slight underestimations, such as in the Danube (-1.2%) and Po (1.7%) basins, to substantial overestimations, as seen in the Adige (32.5%) and Kopru (27.7%) basins. Notably, the Tiber basin exhibits a significant underestimation of -27.3%. These findings highlight the variability in precipitation input

35  accuracy across basins, which can directly affect streamflow simulation. Addressing these biases is crucial, especially in basins like the Adige and Tiber, where large deviations could propagate errors through hydrological models, underscoring the need for bias correction and refinement of precipitation datasets.
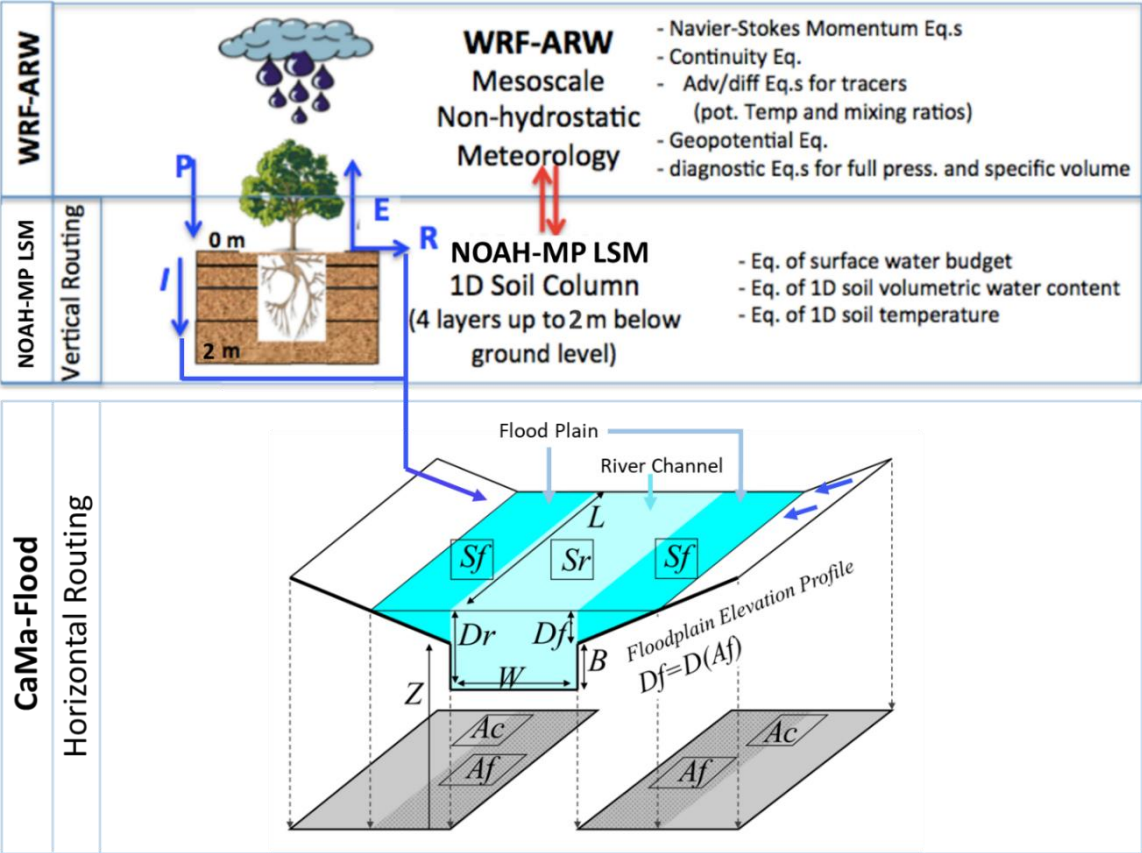
40  **Figure S1: Flowchart of the offline coupling between WRF and CaMa-Flood models (adapted from Yamazaki et al. (2011) and https://www.gewexevents.org/wp-content/uploads/Rasmussen_WRFHydro_USRHP2016.pdf**
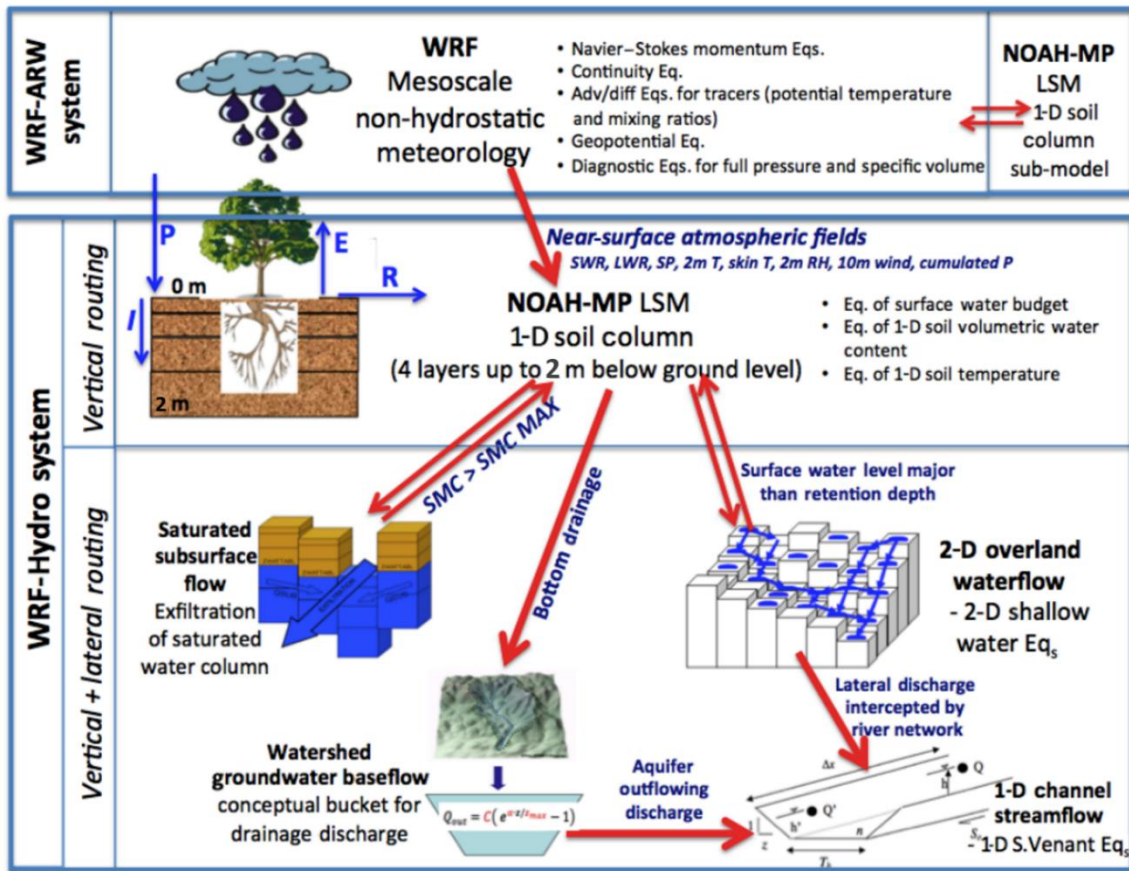
**Figure S2: The schematic structure of the offline coupled WRF/WRF-Hydro model (adapted from Verri et al. (2017)).**
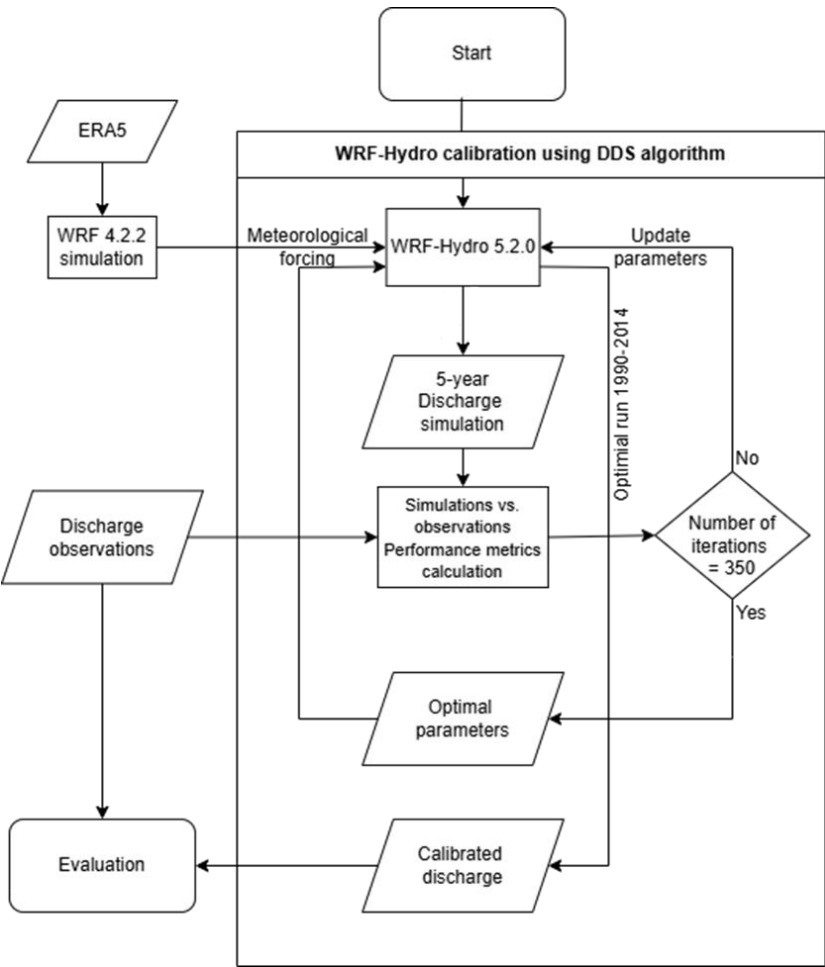
45    **Figure S3: WRF-Hydro calibration flowchart.**
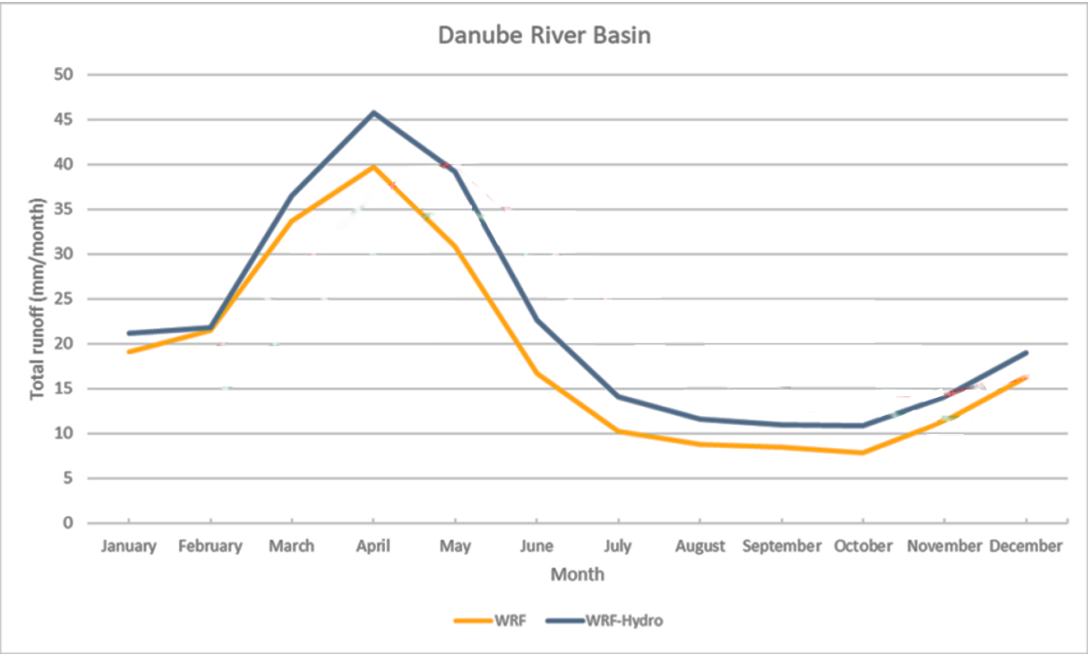
**Figure S4: Mean seasonal cycle of runoff (mm) simulated by WRF and WRF-Hydro, in comparison with ERA5-Land and Noah-MP simulated runoff (Hamitouche et al., 2025).**
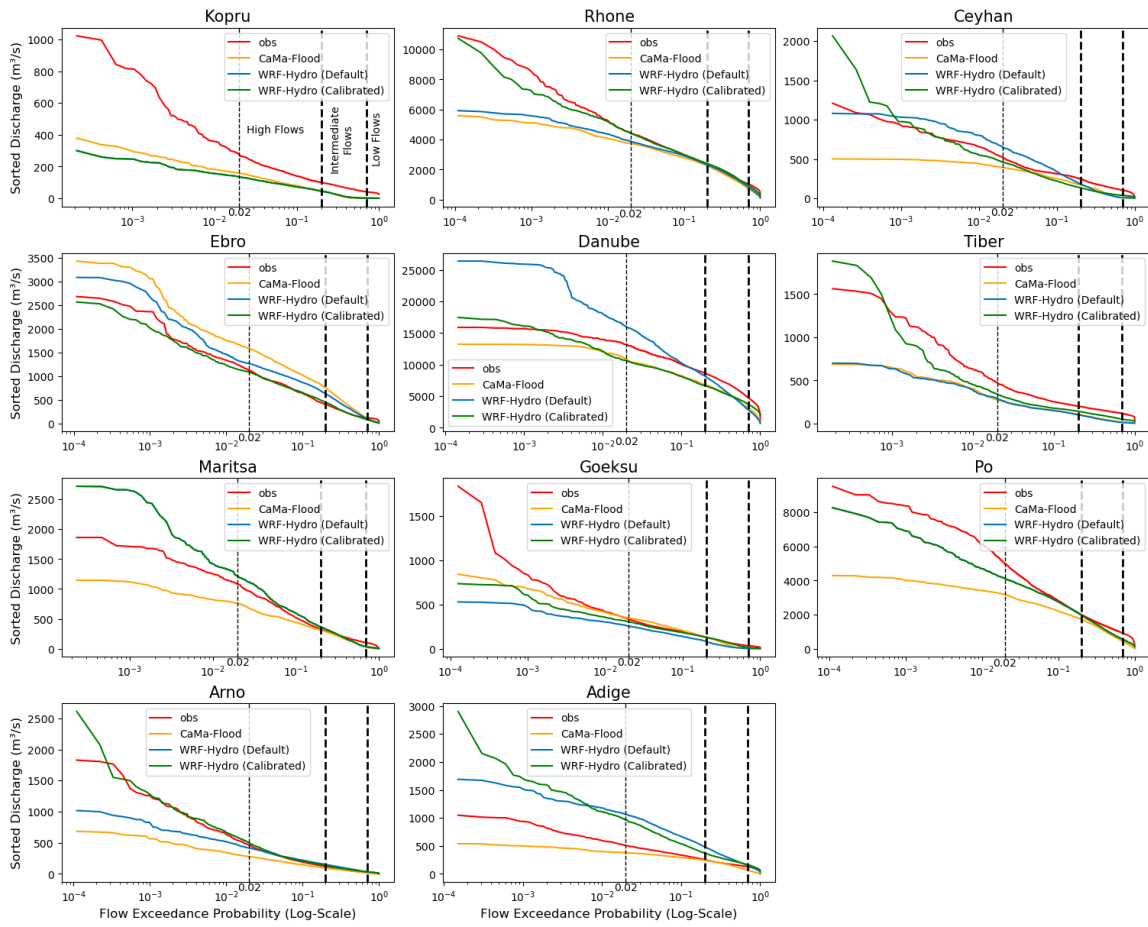
50 **Figure S5: Flow duration curves for each model experiment and basin, with log-scale exceedance probabilities to better visualize the high flows.**
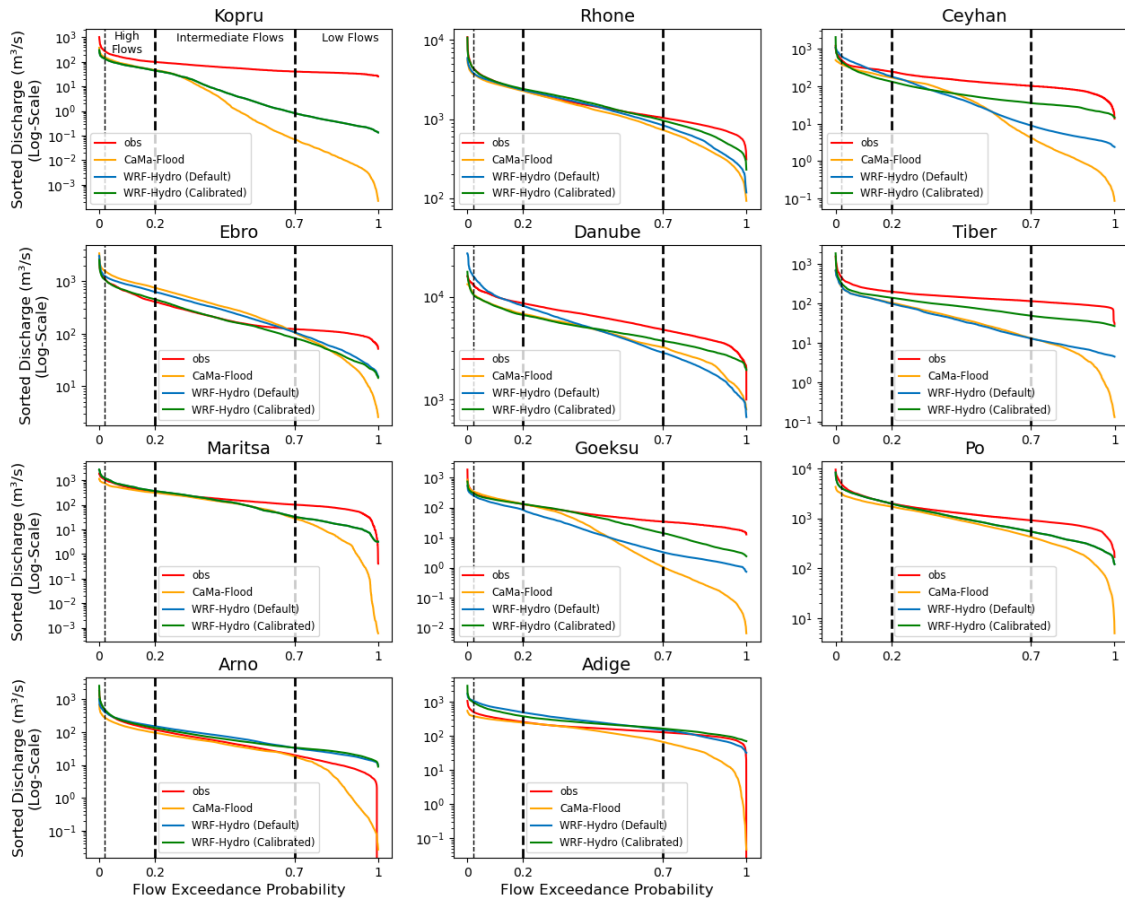
**Figure S6: Flow duration curves for each model experiment and basin, with log-scale discharge values to better visualize the low flows.**

55
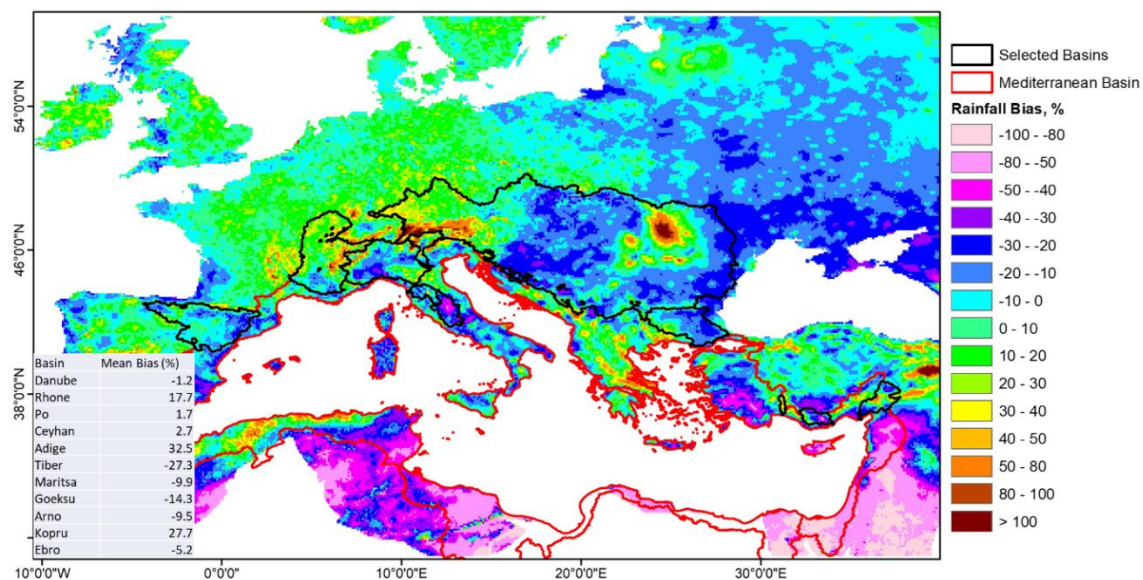
**Figure S7: Distribution of the mean daily rainfall percent bias (100 x (WRF-EOBS)/EOBS)**

60   **Table S1: The main physical parametrizations used by the atmospheric WRF model.**

| Atmospheric model | |
|---|---|
| Model | WRF (v4.2.2) |
| Domain | Med-CORDEX |
| Horizontal resolution | 12 km |
| Domain size | 480 x 350 cells (lon x lat) |
| Vertical resolution | 50 hybrid levels up to 10 hPa |
| Physical time step | 60 s |
| Forcing | ERA5 |
| Relaxation zone | 10 points with an exponential relaxation |
| Microphysics | Morrison (two-moment scheme) |
| Cumulus parametrisation | BMJ |
| Shortwave radiation | RRTMG |
| Longwave radiation | RRTMG |
| Land-surface model | Noah-MP |

**Table S2: Selected Noah-MP Multiphysics Parameterization Options for Physical Processes.**

| Noah-MP multiphysics parameterization | |
|---|---|
| Physical Process | Option |
| Dynamic vegetation option | LAI from lookup table |
| | Maximum vegetation fraction from climatology |
| Canopy stomatal resistance | Ball-Berry |
| Soil moisture factor for stomatal resistance | Noah |
| Runoff | Schaake |
| Surface layer drag coefficient | M-O |
| Frozen soil permeability | Niu and Yang (2006) |
| Super cooled liquid water | Niu and Yang (2006) |
| Radiative transfer | Two-stream applied to vegetated fraction |
| Ground snow surface albedo | CLASS |
| Precipitation partitioning | Jordan (1991) |
| Lower boundary condition for soil temperature | Original Noah |
| Snow/soil temperature time scheme | Semi-implicit with FSNO |
| Glacier treatment | Ice treatment more like original Noah |
| Surface resistance to evap/sublimation | Snow/non-snow split |

65

70

75

80   **Table S3: WRF-Hydro calibration parameters.**

| Physical Process | Parameter | Description | Units | Default value | Range | Calibration scalar multiplier |
|---|---|---|---|---|---|---|
| Soil | bexp | Pore size distribution index | - | 1 | 0.4–1.9 | Yes |
| | smcmax | Saturation soil moisture content (i.e., porosity) | Volumetric fraction | 1 | 0.8–1.2 | Yes |
| | dksat | Saturated hydraulic conductivity | m/s | 1 | 0.2–10 | Yes |
| | rsurfexp | Exponent in the resistance equation for soil evaporation | - | 5 | 1–6 | No |
| Runoff | refkdt | Surface runoff parameter | - | 1 | 0.1–4 | No |
| | slope | Coefficient to modify the drainage out the bottom of the last soil layer | 0–1 | 0.3 | 0–1 | No |
| | retdeprtfac | Multiplier on retention depth limit | - | 1 | 0.1–20,000 | No |
| | lksatfac | Multiplier on lateral hydraulic conductivity | - | 1000 | 10–10,000 | No |
| | ovroughrtfac | Multiplier on 2D overland flow roughness factor | - | 1 | 0.01-1 | No |
| Groundwater | zmax | Maximum conceptual nonlinear reservoir depth | mm | 50 | 10–250 | No |
| | expon | Exponent controlling rate of bucket drainage as a function of depth | - | 3 | 1–8 | No |
| | Coeff | controlling rate of bucket drainage as a function of depth | $m^3/s$ | 0.001 | 0.0001-0.1 | No |
| Vegetation | cwpvt | Canopy wind parameter for canopy wind profile formulation | 1/m | 1 | 0.5–2 | Yes |
| | vcmx25 | Maximum carboxylation at 25°C | $\mu mol/m^2/s$ | 1 | 0.6–1.4 | Yes |
| | mp | Slope of Ball-Berry | - | 1 | 0.6–1.4 | Yes |

| | | | | | conductance relationship | | | |
|---|---|---|---|---|---|---|---|---|
| | hvt | Canopy height | m | 1 | 0.25-1.5 | Yes | | |

**Table S4: Optimal values of calibrated parameters for each river basin.**

| Parameters | Default value | Danube | Rhone | Ceyhan | Adige | Tiber | Goeksu | Arno | Ebro |
|---|---|---|---|---|---|---|---|---|---|
| bexp | 1.000 | 0.480 | 1.881 | 0.435 | 0.424 | 1.503 | 0.959 | 1.848 | 1.892 |
| smcmax | 1.000 | 1.198 | 1.198 | 1.155 | 1.193 | 0.816 | 0.835 | 1.195 | 1.199 |
| dksat | 1.000 | 1.029 | 0.347 | 0.751 | 0.368 | 0.342 | 1.087 | 0.579 | 0.575 |
| rsurfexp | 5.000 | 5.213 | 4.990 | 4.869 | 5.972 | 3.471 | 2.369 | 5.732 | 5.899 |
| refkdt | 1.000 | 3.722 | 1.461 | 3.057 | 3.987 | 1.486 | 3.468 | 3.796 | 1.447 |
| slope | 0.300 | 0.013 | 0.104 | 0.016 | 0.026 | 0.890 | 0.103 | 0.010 | 0.021 |
| retdeprtfac | 1.000 | 5.095 | 8.763 | 9.218 | 3.850 | 0.142 | 9.893 | 0.731 | 4.848 |
| lksatfac | 1000.0 | 959.3 | 3700.3 | 3681.9 | 836.0 | 6606.1 | 6093.3 | 4633.8 | 2194.8 |
| ovroughrtfac | 1.000 | 0.919 | 0.996 | 0.964 | 0.993 | 0.027 | 0.768 | 0.922 | 0.971 |
| zmax | 50.00 | 249.2 | 247.8 | 249.7 | 231.3 | 249.2 | 10.76 | 249.0 | 63.35 |
| expon | 3.000 | 3.075 | 1.930 | 3.339 | 4.453 | 3.308 | 1.082 | 1.003 | 1.401 |
| Coeff | 0.001 | 0.046 | 0.020 | 0.096 | 0.099 | 0.083 | 0.010 | 0.002 | 0.006 |
| cwpvt | 1.000 | 0.548 | 0.533 | 0.596 | 0.513 | 0.542 | 1.952 | 0.760 | 0.530 |
| vcmx25 | 1.000 | 1.004 | 1.006 | 0.648 | 1.368 | 0.641 | 1.400 | 0.816 | 1.147 |
| mp | 1.000 | 1.095 | 1.023 | 0.601 | 1.376 | 0.959 | 1.389 | 1.281 | 1.311 |
| hvt | 1.000 | 0.253 | 0.302 | 1.342 | 0.254 | 0.451 | 0.364 | 0.970 | 0.254 |

85

90

95

100

105

110

**Table S5: Comparison between the runoff from WRF (atmosphere-land model), and both WRF-Hydro default and calibrated for each river basin.**

| Basin | Model | Average total runoff (mm/day) | Ratio subsurface/total runoff |
|---|---|---|---|
| Danube | WRF | 0.615 | 0.824 |
| | WRF-Hydro (Default) | 0.732 (+19.0%) | 0.926 (+12.4%) |
| | WRF-Hydro (Calibrated) | 0.564 (-23.0%) | 0.912 (-10.5%) |
| Rhone | WRF | 1.293 | 0.846 |
| | WRF-Hydro (Default) | 1.558 (+20.5%) | 0.891 (+05.3%) |
| | WRF-Hydro (Calibrated) | 1.216 (-22.0%) | 0.658 (-26.2%) |
| Po | WRF | 1.325 | 0.856 |
| | WRF-Hydro (Default) | 1.626 (+22.7%) | 0.908 (+06.1%) |
| | WRF-Hydro (Calibrated) | 1.626 (±0%) | 0.908 (±0%) |
| Ceyhan | WRF | 0.515 | 0.616 |
| | WRF-Hydro (Default) | 0.623 (+21.0%) | 0.913 (+48.2%) |
| | WRF-Hydro (Calibrated) | 0.375 (-39.8%) | 0.868 (-04.9%) |
| Adige | WRF | 1.722 | 0.879 |
| | WRF-Hydro (Default) | 1.913 (+11.1%) | 0.915 (+04.1%) |
| | WRF-Hydro (Calibrated) | 1.520 (-20.5%) | 0.884 (-03.4%) |
| Tiber | WRF | 0.532 | 0.759 |
| | WRF-Hydro (Default) | 0.595 (+11.8%) | 0.934 (+23.1%) |
| | WRF-Hydro (Calibrated) | 0.883 (+48.4%) | 0.831 (-11.0%) |
| Maritsa | WRF | 0.398 | 0.652 |
| | WRF-Hydro (Default) | 0.462 (+16.1%) | 0.883 (+35.4%) |
| | WRF-Hydro (Calibrated) | 0.462 (±0%) | 0.883 (±0%) |
| Goeksu | WRF | 0.535 | 0.570 |
| | WRF-Hydro (Default) | 0.516 (-03.6%) | 0.928 (+62.8%) |
| | WRF-Hydro (Calibrated) | 0.971 (+88.2%) | 0.963 (+03.8%) |
| Arno | WRF | 0.613 | 0.764 |
| | WRF-Hydro (Default) | 0.918 (+49.8%) | 0.959 (+25.5%) |
| | WRF-Hydro (Calibrated) | 0.613 (-33.2%) | 0.885 (-07.7%) |
| Kopru | WRF | 1.021 | 0.423 |
| | WRF-Hydro (Default) | 1.257 (+23.1%) | 0.930 (+119.9%) |
| | WRF-Hydro (Calibrated) | 1.257 (±0%) | 0.930 (±0%) |

| | | | |
|---|---|---|---|
| Ebro | WRF | 0.433 | 0.799 |
| | WRF-Hydro (Default) | 0.495 (+14.3%) | 0.926 (+15.9%) |
| | WRF-Hydro (Calibrated) | 0.257 (-48.1%) | 0.660 (-28.7%) |